A COMPARISON OF MATERIAL STATE MONITORING TECHNIQUES APPLIED TO RESIN TRANSFER MOULDING

Daniel Griffin[1], Alper Aktas[1], Maria Lodeiro[1], Tim Young[2], Ian Hamerton[3], Ivana Partridge[3]

[1] National Physical Laboratory, Hampton Road, Teddington, TW11 0LW, UK
[2] National Composites Centre, Bristol & Bath Science Park, Emersons Green, Bristol, BS16 7FS, UK
[3] University of Bristol, Queen's Building, University Walk, Clifton, BS8 1TR, UK

Keywords: Resin Transfer Moulding, Cure monitoring, Direct current, Dielectric spectroscopy, Ultrasound, Fibre Bragg grating, Unsaturated polyester resin, Epoxy resin

ABSTRACT

In this study, a combined cure monitoring system development comprising dielectric spectroscopy (DEA), direct current (DC) resistivity, ultrasound, fibre-Bragg gratings (FBG) and temperature sensors for the Resin Transfer Moulding (RTM) process is presented. This system is capable of monitoring cure, 3D flow front, flow rate, pressure and temperature using embedded and tool-mounted sensors. An RTM mould with a heating capability has been designed with sensor ports. In order to assess this multi-sensing approach, some preliminary investigations were performed using a slow curing epoxy (Prime 20 LV) and a slow curing unsaturated polyester (Crystic 701PA) thermoset resin systems. An E-glass fibre multiaxial reinforcement system was used. Two-stage cure monitoring experiments (room temperature cure followed by a post-cure cycle) were performed. The changes in signals indicated flow front arrivals, temperature ramps and state of resins. This paper presents the techniques, multi-sensing approach and preliminary results.

1 INTRODUCTION

The behaviour of liquid thermoset resins and, in particular, their interactions with dry fibre reinforcement are significant contributing factors to process and product variability in Liquid Composite Moulding (LCM) processes, such as resin transfer moulding (RTM) [1]. This stems from the requirement for intimate mixing of resin and reinforcement to produce a composite material, at the same time as the product itself is formed. The combination of these stages into a single manufacturing process generates a broad scope for variability in the quality of the product. Online measurement of resin properties during the process is therefore a key enabler for process optimisation, informing the control of processing conditions to achieve optimal and predictable resin behaviour.

A broad range of suitable cure monitoring techniques have been presented and assessed in the literature, capable of probing properties such as: electrical (e.g. dielectric, direct current) [2], [3], acoustic (e.g. ultrasound) [4], optical (e.g. infrared and Raman spectroscopy) [5], [6], thermal (e.g. thermocouples, thermistors) [7], as well as dimensional variations (e.g. fibre Bragg gratings, pressure sensors) [8], [9]. However, while there is a growing need to evaluate these technologies in realistic manufacturing processes and environments, examples of simultaneous application of such techniques to LCM processes are limited [10], [11].

In this study, a combined monitoring approach, utilising dielectric spectroscopy (DEA), direct current (DC) resistance, ultrasound, fibre Bragg gratings (FBG), and temperature sensors, has been applied to the RTM manufacture of flat panels. Results are presented for two industrial grade, slow curing thermoset resin systems with E-glass multiaxial fibre reinforcement. These are the first in a set that will aim to evaluate the performance and practicalities of using the various monitoring systems with different resin – reinforcement combinations.

2 METHODOLOGY

The RTM setup employed in this work comprises:

- aluminium base mould (sample area: 200 mm x 600 mm) with glass upper mould section and adjustable cavity height (0 – 30 mm),
- oil-heating unit capable of temperatures up to 200 ℃,
- injection machine capable of resin injection pressures up to 3 bar (gauge), with heated resin pot and hose.

Resin enters the mould cavity via a single injection port at one end of the base unit, with a single vent located at the opposite end, and cured samples are demoulded with the aid of an air ejector in the lower half of the mould. The cavity height was set to 3 mm.

The lower half of the mould also contains 11 sensor ports, which were equipped with six pressure sensors, four coaxial electrode sensors, and one interdigitated electrode sensor, as shown in Figure 1.

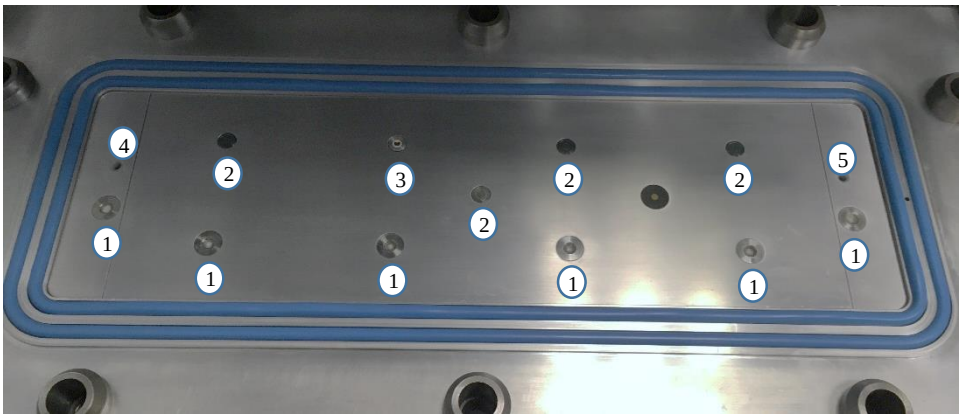

Figure 1: Lower tool configuration, numbered as: (1) pressure sensors, (2) coaxial electrode sensors for flow front detection, (3) interdigitated electrode sensor, (4) resin inlet, (5) resin outlet.

As well as these durable, tool-mounted sensors, an embedded, disposable interdigitated electrode sensor was used to conduct DC resistance measurements between the central plies of the laminate, for comparison with surface measurements from the tool-mounted electrode sensors. A multiplexed FBG fibre optic, also embedded, was employed for resin flow-front, cure (via strain evolution), and temperature measurements. Pulse-echo ultrasound was investigated as a non-intrusive monitoring technique, with the transducer mounted externally on the upper mould.

2.1 DC resistance

Under a static electric field, the electrical resistance of a polymeric material is dominated by the mobility of ionic species within. Changes in the state of polymeric resins during LCM processing that affect ionic mobility can hence be inferred from in-situ resistance measurements [12].

Both tool-mounted coaxial and embedded interdigitated electrode sensors supplied by Synthesites, with integrated Pt100 temperature sensors, were used to probe changes in the resins resistance during the course of the manufacturing process. While the tool-mounted sensor achieved this at the component-tool interface, the embedded sensor placed halfway up the reinforcement stack enabled measurement in the bulk laminate. Three tool-mounted flow sensors were used along the length of the cavity for resin arrival detection. Synthesites OptiMold and OptiFlow data acquisition units were used for cure and flow monitoring respectively, operated via the OptiView software package.

2.2 Dielectric analysis

Dielectric analysis (DEA) probes the response of a material to an applied alternating electric field. In the case of polymeric resins found in fibre reinforced polymer (FRP) composite materials, frequencies across the Hz – MHz range are generally employed [13], [14]. The applied field is attenuated and phase

shifted as it interacts with a polymeric sample, due primarily to induced ionic and dipole motions [15], hence enabling the complex capacitance or impedance of the sample to be measured. From this data, it is possible to determine the complex permittivity of the sample material, i.e. permittivity, ε', and dielectric loss, ε'', which can be used to characterise the materials viscoelastic behaviour.

A durable, tool-mounted interdigitated electrode sensor supplied by ADVISE, with integrated T-type thermocouple, was used to probe the dielectric response of resin at the component-tool interface. Impedance measurements were conducted with a Solartron 1260A frequency response analyser coupled to a Solartron 1296A dielectric interface and controlled with the SMaRT software, enabling measurements up to 1 TΩ. Frequency sweeps were carried out over the frequency range 0.1 Hz – 100 kHz, at 4 or 5 points per decade, for the duration of the manufacturing process, with a minimum measurement duration of 1 second at each frequency.

2.3 Ultrasound

The formation of a highly cross-linked polymer network during the curing stage of any thermoset FRP manufacture process, is accompanied by an evolution in the viscoelastic behaviour of the resin [16]. This evolution can be interrogated via analysis of pressure wave propagation through the material, the underlying principle behind ultrasonic monitoring techniques [17]. In this study, reflection, or pulse-echo, ultrasound was employed to interrogate the interface between the upper tool and the composite laminate, characterised by the discontinuity in acoustic impedance across the interface, as determined by Equation 1 [18]:

$$R = \left(\frac{Z_1 - Z_2}{Z_1 + Z_2}\right)^2 \tag{1}$$

Ultrasonic measurements were conducted using a broadband piezoelectric transducer, centred around 2.25 MHz, positioned centrally on the top of the mould. The transducer was powered by a JSR pulsed signal generator, with data acquisition via a National Instruments PXI-5122 oscilloscope card and LabVIEW software.

2.4 Fibre Bragg gratings

Fibre Bragg gratings enable interrogation of the physical interaction between the resin and the embedded fibre optic, which evolves over the course of the manufacture process. FBGs are produced by periodic alteration of the refractive index of the fibre core to create a grating which reflects light in a specific narrow wavelength range, centred around the characteristic Bragg wavelength, λ_B. Strain applied to a grating causes either elongation or compression of the grating periodicity, and hence a shift in the Bragg wavelength [19].

Applied to FRP composite manufacture processes, the strain caused by flow of resin along an FBG sensor during infusion can be detected and hence used to monitor resin arrival at sensor locations. During resin cure, once the viscosity of the resin begins to increase dramatically due to the extensive cross-linking, an FBG will become strained as the resin shrinks around it, enabling identification of the onset of gelation and the subsequent progress of the reaction to be monitored. Since the Bragg wavelength of an FBG is affected by temperature as well as strain, it is necessary to account for wavelength shifts as a result of temperature changes before strain analysis can be conducted. Here, a grating enclosed in a rigid sheath was employed to isolate the thermal response of the sensors from longitudinal strain developed in the laminate.

A multiplexed fibre optic sensor supplied by SmartFibres, equipped with 4 equally spaced FBGs and one temperature sensor, (isolated FBG), was embedded between the central plies of the preform. The gratings were aligned along the direction of resin flow, and located at the same locations along the mould as the DC flow sensors. The temperature sensor, located at the tip of the fibre optic, was positioned in the centre of the composite, above the tool-mounted dielectric sensor. Sensor interrogation was achieved using a SmartFibres W4 FBG interrogator connected to MicronOptics ENLIGHT software.

3 MATERIALS

For this initial study, industrial grade room temperature, slow curing thermoset resin systems have been used, namely Gurit Prime 20LV epoxy with slow amine hardener (1:0.26 by weight), and Scott Bader Crystic 701PA unsaturated polyester (UP) with Butanox M50 methyl ethyl ketone peroxide (MEKP) catalyst (1:0.01 by volume). For each resin system, the constituent parts were thoroughly mixed together for 5 minutes and degassed for a further 5 minutes prior to injection. The cure profile followed for each of the resins is given in Table 1.

Resin	Initial Cure Temperature (℃)	Duration (hr)	Post-cure Temperature (℃)	Duration (hr)
Prime 20LV *(epoxy)*	Ambient	26	65	3
Crystic 701PA (unsaturated polyester)	Ambient	24	80	3

Table 1: Cure profile applied for each resin system.

Each panel specimen was manufactured with 4 plies of an E-glass multiaxial fibre reinforcement, (810 g/m^2) to produce a laminate with fibre volume fraction, V_f, of 0.42. Marbocote 227CEE mould release agent was applied to the RTM tool prior to each infusion.

4 RESULTS AND DISCUSSION

Results obtained for both resins are presented in this section. Elapsed time is calculated from the time at which the resin components were initially mixed, and temperatures plotted are those recorded by the Pt100 temperature sensor integrated into the tool-mounted DC cure sensor. Temperature sensor outputs are not discussed in the context of cure monitoring since the thin (i.e. 3 mm) laminates, and long, ambient cures profiles minimised any measurable exotherms. The mould fill times were recorded by means of the DC flow sensors and a webcam, which were 19 minutes and 8 minutes for the epoxy and UP resins, respectively. The injection pressure was ~1.5 bar (gauge).

4.1 DC resistance

The results obtained with both embedded and tool-mounted cure sensors are shown in Figure 2a for epoxy, and Figure 2b for unsaturated polyester. As expected, the arrival of resin at the sensor location for all DC sensors was indicated by a sharp reduction in the measured electrical resistance across the electrodes, due to the greater conductivity of the resin compared with the air it displaced.

In the case of the epoxy, a continual increase in log(resistance), LogR, was detected throughout the ambient curing stage (up to 26 hours), as the polymerisation reaction progressed. The linear trend recorded by both sensors during the early hours is indicative of the region prior to resin gelation, in which resistance is expected to correlate directly with resin viscosity [20], whilst viscosity tends to rise exponentially.

The gradual reduction in gradient that is subsequently evident indicates the onset of gelation, as ionic mobility became dominated by the polymer network cross-link density rather than changes in viscosity. Whereas the embedded sensor showed increasing resistance, and hence continued reaction, up until the end of the initial cure stage, the output from the tool-mounted sensor plateaued after 22 hours. This was due to the upper measurement limit of the monitoring system, i.e. 10^{14} Ω, being exceeded, an issue which can arise at lower temperatures. The embedded sensor, which had a larger effective sensing area and hence greater sensitivity due to its interdigitated design, was not affected in the same way. Given the slow speed of reaction at ambient temperature, and associated gradual evolution of physical properties, it was not possible from the data to identify a specific region at which gelation was first observed.

At around 27 hours the post-cure was initiated, during which the mould temperature was ramped up to 65 ℃. A rapid drop in measured resistance was observed as the resin heated up, before a subsequent increase as the rate of reaction, and therefore resin cross-link density, increased. The change of gradient at around 29 - 30 hours, evident particularly for the tool-mounted sensor, could indicate vitrification of the resin, since reaction rate in the glassy state would be diffusion limited and hence greatly reduced. Although interpretation of the monitoring output during the post-cure was complicated due to poor temperature control, as evident in the temperature plot in Figure 2a, it would appear that complete reaction was not achieved since measured resistance continued to increase until the end, whereas the resistance of a non-reactive polymer would be expected to reduce as a result of the gradual temperature rise.

The difference in reaction mechanism is evident from the measurements for the polyester resin shown in Figure 2b, with both embedded and tool-mounted sensors showing minimal resistance variation inside the first 4 hours. Hence the resin viscosity is expected to have evolved little during this period.

From around 4 hours, the embedded sensor measured a continual increase in log(resistance), with no indication of reaching a plateau before the post-cure was initiated at 24 hours. The tool-mounted sensor, however, appeared to show a step change in rate of increase of log(resistance) at 4 hours, to a greater rate than was measured by the embedded sensor. As a result, the difference in measured resistance between the two sensors increased from that point onwards, a trend which was not observed in the case of the epoxy resin. The tool-mounted sensor resistance also approached a plateau just prior to post-cure, which was not seen with the embedded sensor.

It is proposed that the difference between the two sensor outputs during the cure stage may have been caused by the migration of contaminant species to the tool-mounted sensor surface, e.g. reaction by-products, which influenced the measurements of that sensor. Upon demoulding of the laminate, spots of an unidentified residue were present on the surface of the tool-mounted sensors, further supporting this hypothesis.

During the post-cure, both sensors exhibited a similar trend, with a reduction in resistance as temperature increased followed by a sharp increase due to the significant increase in reaction rate at the elevated temperature. The signals then approached a level, signifying slowing of the reaction, possibly due to vitrification.

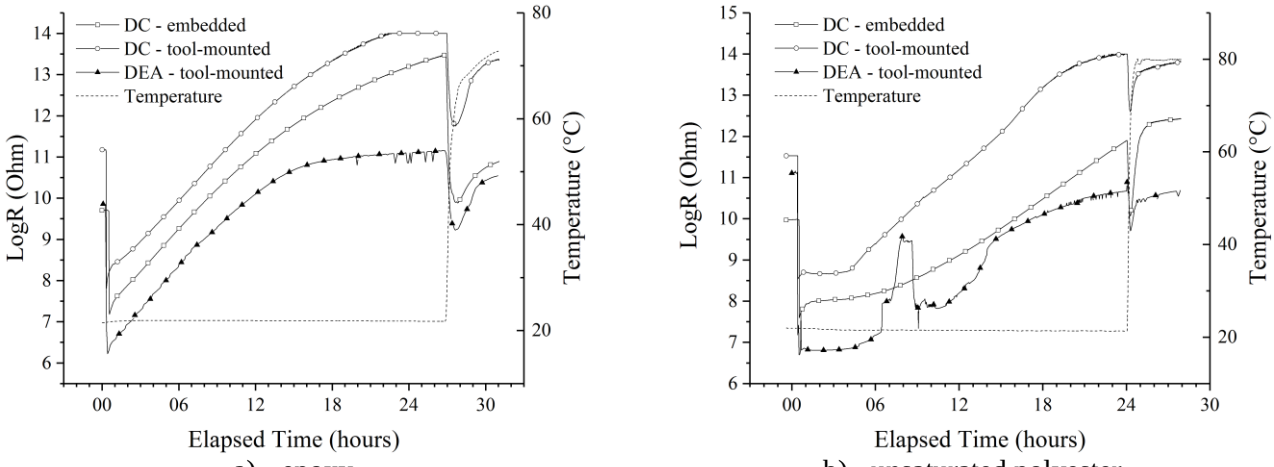

Figure 2: Log(resistance) vs. time elapsed since resin mixing, as measured via DC and DEA monitoring techniques.

4.2 Dielectric analysis

For DEA, the measurement frequency selected for analysis is critical to ensure correct interpretation of the results. In order to determine ionic conductivity, frequencies at which the charge-carrying contributions of ionic species dominate the dielectric response need to be selected. This can be achieved by identification of the frequency at which a peak, or shoulder, is present in the plot of imaginary

impedance against frequency. The dielectric loss at this frequency can then be used to determine ionic conductivity, σ, according to Equation 2 [15]:

$$\sigma = \varepsilon'' \varepsilon_0 \omega \tag{2}$$

Where ε_0 is the vacuum permittivity and ω the angular frequency of the electric field. The inverse conductivity, i.e. resistivity, from this output is compared with DC resistance measurements in Figure 2a (epoxy) and Figure 2b (unsaturated polyester).

In the case of epoxy, a similar trend was observed via DEA as via DC measurements, with resin arrival at the sensor location indicated by a sudden drop in resistivity, followed by a relatively constant increase in LogR due to rising resin viscosity.

However, a much shallower gradient was approached from around 15 hours onwards, which was not observed in DC measurements. Viewed in isolation, this transition might be interpreted as a change in the physical state of the polymer, e.g. vitrification, causing a significant change in reaction rate. In fact, closer analysis revealed that it resulted from the selected measurement frequency reaching the lower bound of the frequency sweep range used, i.e. 0.1 Hz, whilst the optimum measurement frequency for the material, in order to ensure isolation of the contribution from charge-carrying species, continued to transition to lower frequencies. Consequently, imaginary impedance measurements became fixed at this pre-determined boundary frequency, with contributions from dipole motion increasingly challenging the dominance of ionic mobility. An understanding of this transient frequency dependency is therefore crucial to avoid misinterpretation of monitoring output. It should also be noted that, although a wider frequency sweep range could be employed to avoid this issue, the measurement durations required for lower frequency measurements become increasingly large, therefore impacting the temporal resolution of the monitoring technique.

As the post-cure stage was initiated, the observed trend again matched that of the DC measurements. Closer analysis of the monitoring output at around 29 hours supported the proposition that the stepped change in gradient resulted from vitrification of the resin. This was by way of a shoulder present in the real impedance, Z', plot against time, and a knee in the imaginary impedance, Z'', plot against time, (see Figure 3) at higher frequencies, which has previously been proposed as indicating vitrification in Reference [21]. The ability to detect this event is dependent on the sampling interval, which may be limited by the measurement frequency range and spacing employed.

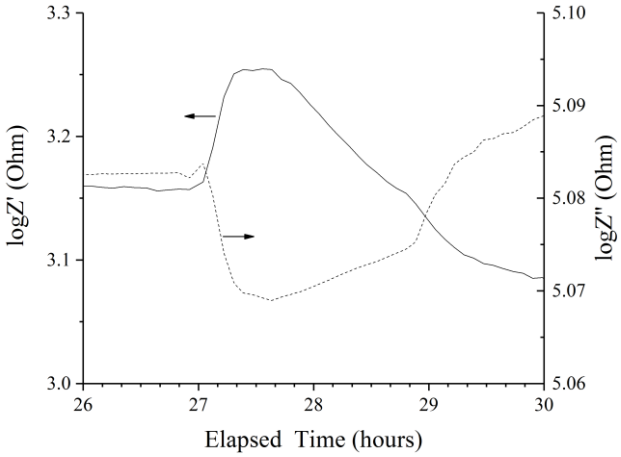

Figure 3: Log(real impedance), logZ', and log(imaginary impedance), logZ'', measured at 100 kHz vs. time elapsed since resin mixing (epoxy).

In the case of unsaturated polyester, again the initial trend matched that observed via DC measurements, dropping upon resin arrival at the sensor location and remaining relatively constant until around 4 hours, when it started to increase gradual. However, from 6 – 10 hours the measurements spiked unexpectedly, which closer inspection revealed was due to the loss of a peak, or optimal, frequency in the imaginary impedance – frequency spectrum. Consequently, the measurement frequency

dropped to the lower bound, i.e. 0.1 Hz, causing a step change in resistivity. It is possible that this response was caused by the migration of contaminant species to the sensor electrodes, as was previously suggested in the case of the DC tool-mounted sensor.

Whilst the resistivity returned to a realistic level from 10 hours, the subsequent trend was different from that observed in either of the DC resistance outputs, and hence it is not clear whether the measurements continued to be detrimentally affected.

4.3 Ultrasound

Only results obtained for the epoxy resin system are presented in this section. The monitoring output, shown in Figure 4, is the peak-to-peak amplitude of the reflected signal from the tool-laminate interface. As expected, resin arrival at the sensor location was detected via a sudden decrease in signal intensity, as the resin displaced air at the interface, reducing the acoustic impedance mismatch and hence reducing the magnitude of the reflected signal.

A peak was observed around 3.5 hours, before the signal amplitude began a steady decline, indicating a reduction in the impedance mismatch between tool and laminate. From around 10 hours onwards, the rate of signal decline increased (see Figure 4b), suggesting a notable change in physical properties of the resin. This may have been an indication of the onset of gelation, with significant network formation increasing the elastic behaviour, and consequently the acoustic impedance, of the resin. The reflected amplitude continued to decrease up until the post-cure stage was initiated at around 27 hrs, suggesting continued reaction until that point.

During the temperature ramp, the signal amplitude increased significantly. This was most likely due to a greater effect of temperature on the impedance of the gelled resin than that of the solid glass mould, an effect which would be exacerbated by thermal lag in the thick mould. At around 29 – 30 hours, a maxima was evident, which coincided with the proposed point of resin vitrification as suggested by electrical measurements.

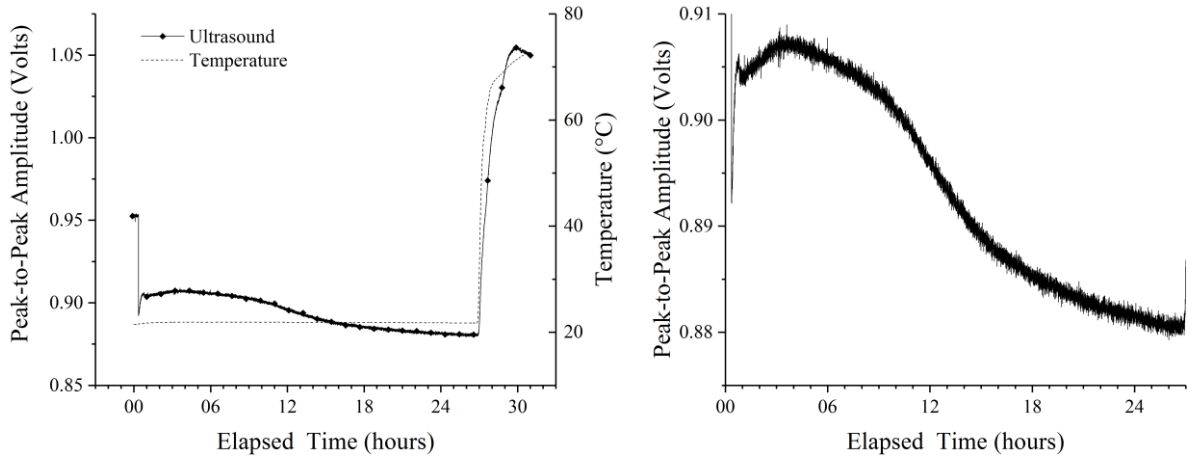

a) Full cure cycle b) Ambient cure cycle (up to 27 hours)

Figure 4: Peak-to-peak amplitude of the reflected ultrasound signal from the tool-laminate (epoxy) interface vs. time elapsed since resin mixing.

4.4 Fibre Bragg gratings

In the data presented in Figure 5a (epoxy) and Figure 5b (unsaturated polyester), Bragg wavelength shifts have been calculated relative to values at t = 55 and t = 58 minutes respectively, determined to be points at which the signals had stabilised after resin injection was stopped and the flow-induced compression of the gratings had relaxed.

During cure under isothermal conditions, it is expected that minimal wavelength shift should be observed prior to gelation since shrinkage in the liquid resin is unable to transfer strain to the solid fibre. As the resin gels around the FBG, mechanical interaction between the two should increase, enabling

compressive strain evolution, i.e. negative $\Delta\lambda$, in the fibre as the resin continues to shrink. This behaviour was evident in the case of the unsaturated polyester (Figure 5b): negligible wavelength variation was observed between the end of injection and 4 hours, from which point fluctuations began to occur across all four and an overarching trend towards negative wavelength shift (i.e. compressive strain) by the end of the ambient cure stage (~ 24 hours) was exhibited. Step changes that occurred between 4 – 10 hours suggest relief of compressive strain in the gratings via slippage at the resin-FBG interface.

However, in the case of the epoxy (Figure 5a), no such trend was evident, each FBG exhibiting a different strain evolution, with no clear indication of the onset of gelation. It is likely that this was due the presence of the multiaxial reinforcement counteracting the resin shrinkage, which is expected to be less severe than for the unsaturated polyester.

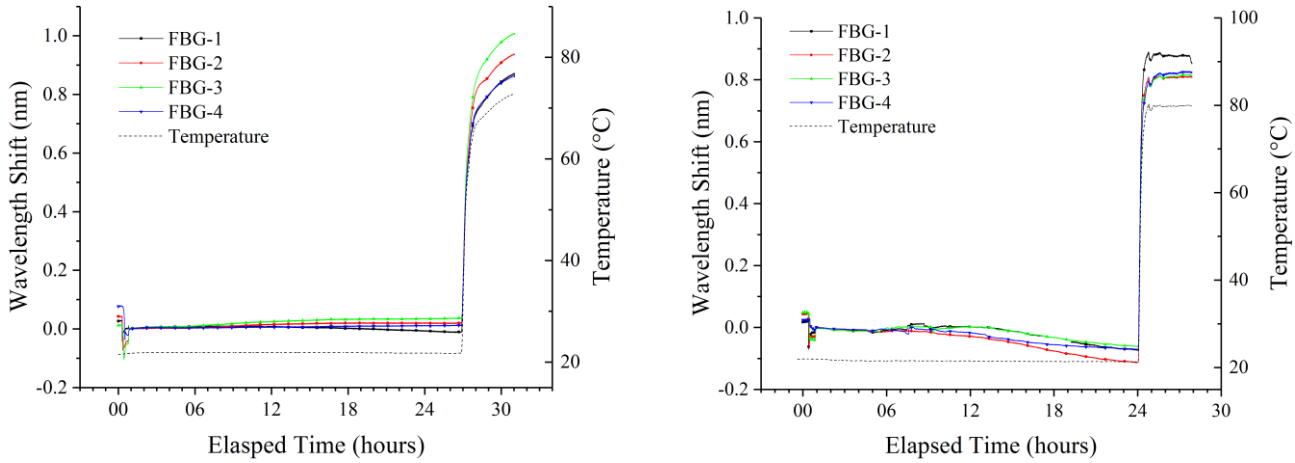

a) epoxy b) unsaturated polyester

Figure 5: Bragg wavelength shifts vs. time elapsed since resin mixing.

Upon initiation of the post-cure stage, the thermal expansion of the fibre optic and laminate caused elongation of the gratings and a significant positive wavelength shift for all gratings. For the epoxy, since no isothermal post-cure temperature was achieved, sensitivity to further resin shrinkage, indicative of continued reaction, was reduced by continuous thermal expansion. For the unsaturated polyester, again wavelength shifts were seen to closely track temperature fluctuations due to the effects of thermal expansion and contraction. Correction for thermal expansion should enable wavelength shifts due to resin cure to be determined, however, this is not trivial since the thermal expansion coefficient of the resin evolves during the cure.

5 CONCLUSIONS AND FUTURE WORK

DC resistance, DEA, ultrasound and FBGs are common in-situ cure monitoring techniques for LCM manufacturing processes. Although they have found applications, none of these have fully been adopted by industry, for reasons such as monitoring capability, material compatibility (e.g. with carbon fibres), mould integration, design issues and cost. There are comparative studies in the literature, but none of them has combined and simultaneously used these to the best knowledge of the authors.

This work has focused on the development of a multi-sensing thermoset resin cure monitoring system for the RTM process, which consisted of DC, DEA, ultrasound, FBG and temperature (thermocouples and isolated FBG) measurement systems. In the experiments, embedded (disposable) DC sensors were used for cure monitoring within the laminate, and pressure sensors, flow sensors and a camera were used to monitor the wetting stage. An RTM mould with a heating capability up to 200°C has been designed with ports to accommodate the embedded and tool-mounted sensors.

The aim has been to build a system, which is capable of monitoring thermoset resin cure simultaneously in an RTM mould in order to compare the reliability, robustness, repeatability and outputs of these most common techniques. On completion of this system, preliminary investigations have been performed using slow curing thermoset resin systems.

DC resistance measurements followed the progress of the polymerization throughout the ambient cure stage, with the exception of the tool-mounted sensor in the case of the epoxy resin system. In that instance, the resistance towards the end of the initial cure exceeded the upper measurement limit of the system (10^{14} Ω). This highlighted the importance of sensor design, and associated sensitivity, for low temperature applications.

DEA measurements were also affected by the low (i.e. ambient) cure temperatures, in that the optimal measurement frequency, required in order to isolate the contributions of charge-carrying species to imaginary impedance, transitioned beyond the lower bound of the frequency sweep range used (0.1 Hz). This resulted in a potentially misleading monitoring output. A wider frequency range could mitigate this problem, but may also reduce the temporal resolution of the monitoring system, due to the inherent longer measurement durations required at lower frequencies.

In the case of the unsaturated polyester resin system, both coaxial (DC) and interdigitated (DEA) electrode tool-mounted sensors appeared to be affected during the process. Following laminate demoulding, evidence of liquid contaminant migration to the sensor surfaces was found. The identity of contaminant species was not determined but was thought to be unreacted monomer or reaction by-products since the same was not seen for the epoxy resin.

Pulse-echo ultrasound tracked evolution of the laminate acoustic impedance and the tool-interface during the process. A change in gradient of the reflected ultrasound intensity was proposed as the possible onset of gelation, whilst a maxima evident during post-cure coincided with the proposed point of vitrification from electrical measurements.

No clear trend in strain development was observed from FBG monitoring for the epoxy resin system, probably as a result of the minimal resin shrinkage expected for epoxy resin, coupled with the presence of reinforcement along the axis of the gratings, able to react resin shrinkage. On the other hand, monitoring of the unsaturated polyester resin identified a point at which signals from the 4 sensors began to diverge, indicating increased mechanical interaction of the gratings with their local environments, likely to be caused by the onset of gelation. An overall compression during the ambient cure stage was also evident for all 4 sensors, attributed to the greater resin shrinkage expected for unsaturated polyester resin compared with epoxy resins.

The work presented here represents the initial stages of a practical evaluation of material state monitoring systems applied to RTM fibre-reinforced polymer manufacture. The results obtained for resins of different polymer chemistry, namely amine cured epoxy and catalyzed unsaturated polyester, have been discussed, with E-glass fibre reinforcement. Cure kinetics and viscosity models are needed to understand these outputs and these will be studied for these two resins and future resin systems. The next stages of work will consider higher curing temperature epoxy resins, both untoughened and toughened, as well as a bismaleimide (BMI) resin, and changing from E-glass to carbon fibre reinforcement.

ACKNOWLEDGEMENTS

This research is supported by one of the National Physical Laboratory's core programme funded by the UK's Department for Business, Energy & Industrial Strategy (BEIS). The authors would also like to acknowledge the Engineering and Physical Sciences Research Council (EPSRC) through the Industrial Doctorate Centre in Composites Manufacture [EP/K50323X/1] and Scott Bader for supplying the unsaturated polyester resin.

REFERENCES

[1] T. S. Mesogitis, A. A. Skordos, and A. C. Long, "Uncertainty in the manufacturing of fibrous thermosetting composites: A review," *Compos. Part Appl. Sci. Manuf.*, vol. 57, pp. 67–75, Feb. 2014.

[2] U. K. Vaidya, N. C. Jadhav, M. V. Hosur, J. W. G. Jr, and B. K. Fink, "Assessment of flow and cure monitoring using direct current and alternating current sensing in vacuum-assisted resin transfer molding," *Smart Mater. Struct.*, vol. 9, no. 6, p. 727, 2000.

[3] M. C. Kazilas and I. K. Partridge, "Exploring equivalence of information from dielectric and calorimetric measurements of thermoset cure—a model for the relationship between curing temperature, degree of cure and electrical impedance," *Polymer*, vol. 46, no. 16, pp. 5868–5878, Jul. 2005.

[4] E. Schmachtenberg, J. Schulte zur Heide, and J. Töpker, "Application of ultrasonics for the process control of Resin Transfer Moulding (RTM)," *Polym. Test.*, vol. 24, no. 3, pp. 330–338, May 2005.

[5] G. R. Powell, P. A. Crosby, D. N. Waters, C. M. France, R. C. Spooncer, and G. F. Fernando, "In-situ cure monitoring using optical fibre sensors - a comparative study," *Smart Mater. Struct.*, vol. 7, no. 4, p. 557, 1998.

[6] L. Merad *et al.*, "In-situ monitoring of the curing of epoxy resins by Raman spectroscopy," *Polym. Test.*, vol. 28, no. 1, pp. 42–45, Feb. 2009.

[7] G. Tuncol, M. Danisman, A. Kaynar, and E. M. Sozer, "Constraints on monitoring resin flow in the resin transfer molding (RTM) process by using thermocouple sensors," *Compos. Part Appl. Sci. Manuf.*, vol. 38, no. 5, pp. 1363–1386, May 2007.

[8] E. Chehura, A. A. Skordos, C.-C. Ye, S. W. James, I. K. Partridge, and R. P. Tatam, "Strain development in curing epoxy resin and glass fibre/epoxy composites monitored by fibre Bragg grating sensors in birefringent optical fibre," *Smart Mater. Struct.*, vol. 14, no. 2, pp. 354–362, Apr. 2005.

[9] C. D. Fratta, "Investigation of a cost-effective system for on-line flow monitoring and quality control in resin transfer molding," in *20th International Conference on Composite Materials*, Copenhagen, 2015, pp. 5207–2.

[10] R. Meier, S. Zaremba, F. Springl, K. Drechsler, F. Gaille, and C. Weimer, "Online process monitoring systems–benchmark and test study," in *11th International Conference on Flow Processes in Composite Materials*, Auckland, 2012.

[11] G. Chiesura *et al.*, "RTM Production Monitoring of the A380 Hinge Arm Droop Nose Mechanism: A Multi-Sensor Approach," *Sensors*, vol. 16, no. 6, Jun. 2016.

[12] Y. A. Tajima, "Monitoring cure viscosity of epoxy composite," *Polym. Compos.*, vol. 3, no. 3, pp. 162–169, Jul. 1982.

[13] J. W. Lane, J. C. Seferis, and M. A. Bachmann, "Dielectric studies of the cure of epoxy matrix systems," *J. Appl. Polym. Sci.*, vol. 31, no. 5, pp. 1155–1167, Apr. 1986.

[14] D. E. Kranbuehl, S. E. Delos, M. S. Hoff, M. E. Whitham, L. W. Weller, and P. D. Haverty, "Dynamic dielectric analysis for nondestructive cure monitoring and process control," in *Review of Progress in Quantitative Nondestructive Evaluation*, Springer, 1987, pp. 1297–1306.

[15] J. Mijović, J. Kenny, A. Maffezzoli, A. Trivisano, F. Bellucci, and L. Nicolais, "The principles of dielectric measurements for in situ monitoring of composite processing," *Compos. Sci. Technol.*, vol. 49, no. 3, pp. 277–290, Jan. 1993.

[16] C. W. Macosko, "Rheological changes during crosslinking," *Br. Polym. J.*, vol. 17, no. 2, pp. 239–245, 1985.

[17] P. A. Gibbs, "Ultrasonic cure measurements during the processing of an unsaturated polyester dough moulding compound," in *Designed for Life: Composites '94*, 1994, pp. 7–16.
[18] B. B. Djordjevic, "Ultrasonic cure monitoring," in *AIP Conference*, 1999, vol. 497, pp. 388–393.
[19] P. Parlevliet, E. Voet, H. Bersee, and A. Beukers, "Process Monitoring with FBG sensors during vacuum infusion of thick composite laminates," in *Proceedings of the 16th International Conference of Composite Materials, Kyoto, Japan*, 2007, vol. 813.
[20] T. Koike, "Relationship between melt viscosity and dielectric relaxation time for a series of epoxide oligomers," *J. Appl. Polym. Sci.*, vol. 47, no. 3, pp. 387–394, Jan. 1993.
[21] A. A. Skordos and I. K. Partridge, "Impedance cure and flow monitoring in the processing of advanced composites," in *International Conference for Manufacturing of Advanced Composites*, Belfast, UK, 2001.